Publication II

Konstantin S. Kostov, Jukka-Pekka Sjöroos, Jorma J. Kyyrä, and Teuvo Suntio. 2004. Selection of power filters for switched mode power supplies. In: Proceedings of the 2004 Nordic Workshop on Power and Industrial Electronics (NORPIE 2004). Trondheim, Norway. 14-16 June 2004. 7 pages.

Selection of Power Filters
for Switched Mode Power Supplies

Konstantin S. Kostov, Jukka-Pekka Sjöroos, Jorma J. Kyyrä, and Teuvo Suntio

Abstract - **Power filter manufacturers provide Insertion Loss (IL) measurement data for their products. These are usually 50 Ω / 50 Ω and sometimes the so-called "approximate worst case measurements". The aim of this work is to find out which of these data should be considered when selecting an input filter for a switched mode power supply. The results show that, the actual common mode attenuation of a filter operating with a buck converter is almost same as the IL data with 0.1 Ω / 100 Ω source and load impedance, whereas the actual differential mode IL is approximately same as the IL data for 100 Ω / 0.1 Ω conditions.**

Index Terms—**Electromagnetic compatibility, Electromagnetic interference, Insertion Loss, Power filters, Switched mode power supplies.**

I. INTRODUCTION

POWER line filter manufacturers provide *Insertion Loss* (IL) measurements for their products. Most often these are measured with 50 Ω source and load impedance. In practice, however, it is very unlikely that a power filter will operate under such conditions. Source and load impedance mismatch is typical in the field of power electronics [1] and that is why 50 Ω / 50 Ω IL measurements are often criticized [2], [3].

In addition to the standard IL measurements, some filter manufacturers also provide measurements with 0.1 Ω / 100 Ω and 100 Ω / 0.1 Ω source and load impedances. These so-called "approximate worst case measurements" are based on CISPR 17 and their aim is to provide IL data, which are closer to the real world operation [3].

This work is concerned with dc-dc *switched mode power supplies* (SMPS), which are unavoidably sources of *electromagnetic interference* (EMI). Due to the switching, a SMPS draws pulsating current from the dc power line, which causes *differential mode* (DM) conducted emissions. The switching actions over the parasitic capacitance to ground, on the other hand, cause *common mode* (CM) conducted EMI from the SMPS.

The source and load impedance mismatch is the major problem when evaluating the effectiveness of an input filter. The DM noise source impedance depends on the type of the converter and its components, whereas the CM noise source impedance depends on parasitic elements. That is why the CM EMI levels may differ depending on the particular PCB technology, components and layout.

The load impedance for the conducted EMI in operating conditions depends on the power line impedance, which can vary widely. Fortunately, it can be measured, if necessary. As far as the EMC compliance tests are concerned, the *line impedance stabilization network* (LISN) provides a well defined 50 Ω load for the conducted emissions.

II. INSERTION LOSS

A. Conducted Emissions Measurements

Conducted emissions measurements for single phase, including dc applications, are carried out using two LISN circuits as shown in Fig. 1. Noise levels are measured separately for line and neutral. If any of them fails to comply with the standard, the equipment is not EMC compatible.

Due to the high impedance of the LISN's inductances the DM noise current flows through two 50 Ω resistors in series, resulting in 100 Ω total load. On the other hand, for the CM EMI current, the two 50 Ω resistors are in parallel, resulting in 25 Ω total load for the CM noise.

The required IL from an EMI filter is sometimes described

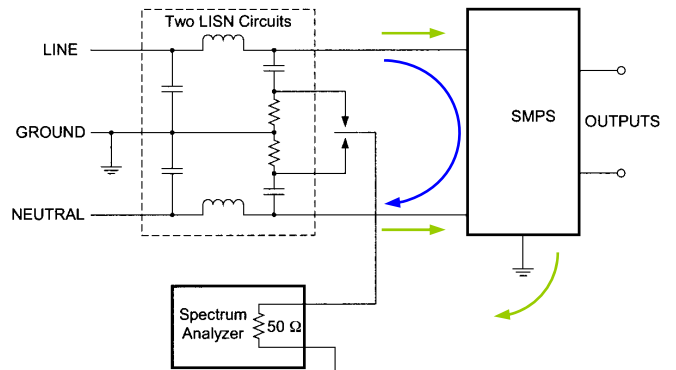K. S. Kostov is with the Power Electronics Laboratory, Helsinki University of Technology, P.O.Box 3000, FIN-02015 HUT, Finland (phone: +358 9 451 4968; fax: +358 9 451 2432; e-mail: Konstantin.Kostov@hut.fi)

J.-P. Söroos, is with the Power Electronics Laboratory, Helsinki University of Technology, P.O.Box 3000, FIN-02015 HUT, Finland. (e-mail: jsjoroos@cc.hut.fi).

J. J. Kyyrä is with the Power Electronics Laboratory, Helsinki University of Technology, P.O.Box 3000, FIN-02015 HUT, Finland (e-mail: Jorma.Kyyra@hut.fi).

T. Suntio is with the Institute of Power Electronics, Tampere University of Technology, P.O.Box 692, FIN-33101 Tampere, Finland (e-mail: teuvo.suntio@tut.fi).
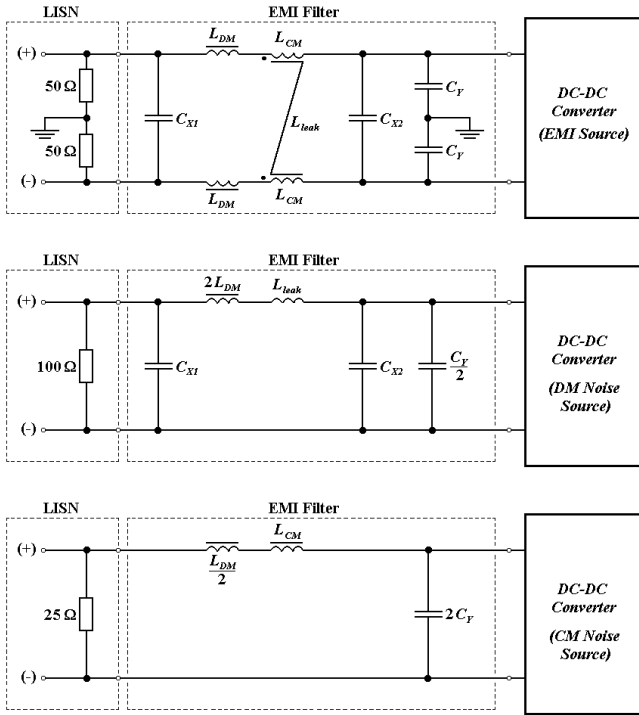
Fig. 1. Measuring conducted EMI from a dc-dc SMPS using two LISNs.

Fig. 2. a) A typical π-filter configuration with its components. b) Equivalent circuit for DM components. c) Equivalent circuit for CM components.

as the difference between the measured EMI from the SMPS and the conducted EMI limits specified in the standards. Indeed, that difference is the required attenuation, but that is the attenuation of both DM and CM. It is important to know in what proportion these EMI components are, in order to choose a filter, which will perform adequately. For example, if the EMI is mostly CM and filter's CM IL too small, the filter will fail to attenuate the noise under the specified limits. Therefore, information about the level of each noise component is crucial for EMI filter selection.

B. EMI Filter Topology and Equivalent Circuits

EMI filter manufacturers usually use π-configuration, as e.g. that in Fig. 2a). They often omit the DM inductor and use only a CM choke. One reason for this is the limited size of Y-capacitors due to safety restrictions on the allowed leakage current. Thus, the burden of CM attenuation is placed mostly on the CM inductor, which can have quite large value. Another reason is that X-capacitors can be as large as possible and instead of using another bulky DM choke, one can rely on the leakage inductance of the CM choke, which is always present and in some cases can be intentionally increased [2].

Considering only DM noise, the π-filter in Fig. 2a) is equivalent to the π-filter in Fig. 2b). On the other hand, for the CM currents, the equivalent is the L-filter in Fig. 2c), unless the Y-capacitors are connected at both ports of the filter.

The EMI filter built for this study has π-configuration with CM choke only, i.e. the $L_{DM} = 0$ H in Fig. 2 and in the following calculations.

C. DM Noise Attenuation

A chain parameter [4] based method for calculation of the

IL provided by a passive filter was presented in [5]. According to [5] the DM noise attenuation of a π-filter is:

$$IL_{DM} = 20 \cdot \lg \frac{\frac{c_{11} \cdot Z_{DM,load} + c_{12}}{Z_{DM,source}} + c_{21} \cdot Z_{DM,load} + c_{22}}{1 + \frac{Z_{DM,load}}{Z_{DM,source}}} \quad (1)$$

Where c_{11}, c_{12}, c_{21}, and c_{22} are the chain parameters of the DM filter, which is the π-filter in Fig. 2b). In the DM IL data, provided by filter manufacturers, the DM load and source impedances are equal to 50 Ω, i.e. $Z_{DM,load} = Z_{DM,source} = 50$ Ω. In LISN measurements $Z_{DM,load} = 100$ Ω and $Z_{DM,source}$ is unknown. It depends on SMPS's topology and components.

As shown in [5], the chain parameters of a π-filter are:

$$\mathbf{C} = \mathbf{C_1}\mathbf{C_2}\mathbf{C_3} = \begin{bmatrix} 1 & 0 \\ Y_1 & 1 \end{bmatrix}\begin{bmatrix} 1 & Z_2 \\ 0 & 1 \end{bmatrix}\begin{bmatrix} 1 & 0 \\ Y_3 & 1 \end{bmatrix}$$

$$\mathbf{C} = \begin{bmatrix} c_{11} & c_{12} \\ c_{21} & c_{22} \end{bmatrix} = \begin{bmatrix} 1 + Z_2Y_3 & Z_2 \\ Y_1 + Y_1Z_2Y_3 + Y_3 & 1 + Y_1Z_2 \end{bmatrix} \quad (2)$$

Where Y_1, Z_2 and Y_3 are:

$$Y_1 = \frac{1}{Z_{CX2}} + \frac{1}{2 \cdot Z_{CY}} \quad Z_2 = 2 \cdot Z_{DM} + Z_{CM,leak} \quad Y_3 = \frac{1}{Z_{CX1}} \quad (3)$$

All impedances in (3), whether they are X-, or Y-capacitors, or any of the inductors, can be obtained by measurements or from component manufacturer's data sheets, except the leakage inductance of the CM choke, which can only be measured.

D. CM Noise Attenuation

Similarly to the DM, the IL for CM EMI is:

$$IL_{CM} = 20 \cdot \lg \frac{\frac{c_{11} \cdot Z_{CM,load} + c_{12}}{Z_{CM,source}} + c_{21} \cdot Z_{CM,load} + c_{22}}{1 + \frac{Z_{CM,load}}{Z_{CM,source}}} \quad (4)$$

In CM IL measurements again $Z_{CM,load} = Z_{CM,source} = 50$ Ω, whereas in LISN measurements $Z_{CM,load} = 25$ Ω, as explained earlier and shown in Fig. 2c), and $Z_{CM,source}$ is unknown.

The CM noise source is different from the DM EMI source. The CM noise source impedance is the parasitic impedance to ground. Any attempt to model the CM EMI is further complicated by the fact that the CM current does not flow through ground only in the direction of the power line (or LISN). Part of it flows through the ground to the SMPS's load. How much CM current will flow in each direction depends on the ground resistances, making the modeling of the CM noise source a difficult task.
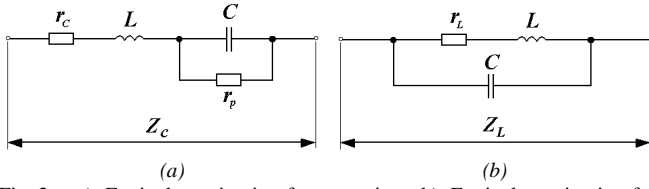
Fig. 3. a) Equivalent circuit of a capacitor. b) Equivalent circuit of an inductor.

The chain parameters for the CM equivalent circuit are:

$$\mathbf{C} = \mathbf{C_1 C_2} = \begin{bmatrix} 1 & 0 \\ Y_1 & 1 \end{bmatrix} \begin{bmatrix} 1 & Z_2 \\ 0 & 1 \end{bmatrix} = \begin{bmatrix} 1 & Z_2 \\ Y_1 & Y_1 Z_2 + 1 \end{bmatrix} = \begin{bmatrix} c_{11} & c_{12} \\ c_{21} & c_{22} \end{bmatrix}$$ (5)

$$Y_1 = \frac{2}{Z_{CY}} \quad Z_2 = Z_{CM} + \frac{Z_{DM}}{2}$$

All impedances in (5) can be measured or calculated from components' datasheets. Then the chain parameters can be inserted in (4) to obtain the CM attenuation for different noise source and load impedances.

III. FILTER COMPONENTS

A. Capacitors

If capacitor's nonlinearities are ignored, it can be modeled by an equivalent circuit [1] as the one shown in Fig. 3a). Then the impedance of a capacitor is:

$$Z_C = r_C + j\omega L + \frac{r_p}{1 + j\omega r_p C}$$ (6)

Both X-capacitors in the EMI filter built for this work are 100 nF. The Y-capacitors are 4.7 nF. All information for these capacitors, as used in the theoretical calculations, is in Table I. It was obtained from manufacturer's datasheets [6] and [7]. There are also the data for the electrolytic capacitor [8] connected across the input of the buck converter. This capacitor could be considered to be a part of the input filter. However, we view it as a part of the converter, because it was kept in the EMC measurements without EMI filter. The reason was that without a large enough electrolytic capacitor buck converter's stable operation could not be guaranteed.

With these values the impedances of the X- and Y-capacitors were calculated according (6). The resulting capacitor impedances are shown in Fig. 4a).
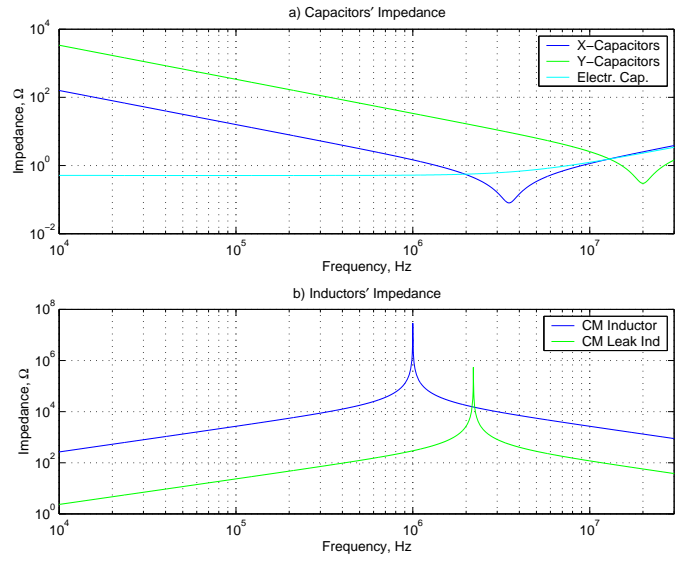

Fig. 4. Theoretical impedances of the: a) capacitors b) inductors used in the EMI filter.

B. Inductors

Fig. 3b) shows the equivalent circuit of an inductor [1]. According it the impedance of an inductor is:

$$Z_L = \frac{r_L + j\omega L}{1 - \omega^2 LC + j\omega r_L C}$$ (7)

The accuracy of the model in Fig. 3b) with the corresponding impedance (7) is not as certain as the capacitor's model. Even in a single choke, the parasitic capacitance is distributed between the turns, resulting in a more complex frequency behavior. Moreover, the EMI suppression inductors have two, or more chokes – one for each conductor. The coupling between the chokes determines whether the inductor is DM or CM. The simple equivalent circuit in Fig. 3b) does not take into account the coupling effects between the chokes.

In the EMI filter built for this work only a CM inductor was used. The inductance and resistance values used in the theoretical calculation are shown in Table II. They are taken from manufacturer's data sheets [9]. The parasitic capacitance is not given in those data sheets, but was calculated from the choke's *self-resonant frequency* (SRF), which was 1 MHz in manufacturer's attenuation curves. In accordance with (7), the theoretical impedance of the choke is shown in Fig. 4b).

TABLE I
CAPACITORS [6], [7], [8].

	C	L	r_C	r_p
X-capacitor	100 nF	20.7 nH	80 mΩ	15000 MΩ
Y-capacitor	4.7 nF	13.5 nH	300 mΩ	15000 MΩ
Electr. Cap.	220 μF	18.0 nH	510 mΩ	-

Tolerance: +20 % -10 % for X- and Y-capacitors; ±20 % for the electrolytic capacitor.

TABLE II
CM CHOKE [9].

	L	C	r_L
RN114-2/02	4.2 mH / path	6.03 pF	102 mΩ / path

Inductance tolerance: +50 %, -30 %
Resistance tolerance: ±15 %, -10 %
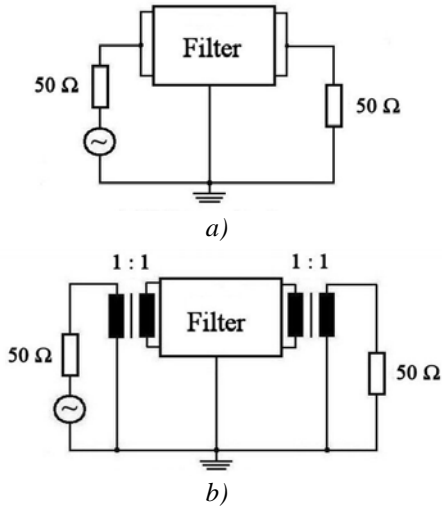
Fig. 5. Insertion loss measuring principle: a) CM (asymmetrical) IL. b) DM (symmetrical) IL.
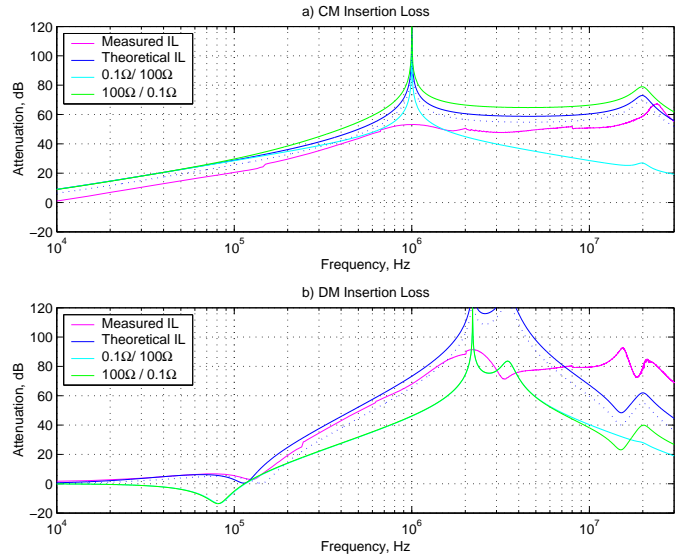

Fig. 6. The measured IL curves are only for the standard $50\,\Omega\,/\,50\,\Omega$ conditions. The other IL curves are theoretically calculated for source and load impedances as given in the legend.

Unfortunately, there is no information about the choke's leakage inductance. It was measured to be 37 µH. The series resistance used for the model of the leakage inductor is twice the resistance per path, i.e. 204 mΩ. The SRF of the leakage inductor model was assumed to be 2.2 MHz to match a peak in the measured DM IL, which is shown later. Fig. 4b) shows the theoretical impedance of the leakage inductor, assuming it can be modeled with the equivalent circuit in Fig. 3b). The leakage inductor model is the most uncertain one from the theoretical models and probably the main reason for the discrepancy between the measured and calculated DM IL shown later.

IV. CALCULATED AND MEASURED INSERTION LOSS

A. CM Insertion Loss

The $50\,\Omega\,/\,50\,\Omega$ CM IL measurements were carried out according to Fig. 5a) as described in [10], using EMI test receiver ESCS 30 from ROHDE & SCHWARZ [11]. The results for the above-described filter are plotted in Fig. 6a). In the same Figure, there are also the theoretically calculated CM IL curves for the standard conditions, i.e. $50\,\Omega\,/\,50\,\Omega$. The dotted line is the theoretically calculated IL for $50\,\Omega\,/\,50\,\Omega$, but with component values reduced by the allowed tolerances in accordance with components' data sheets. It shows how much the IL may drop in theory, due to component's variations.

The measured CM IL is lower, but very close to the theoretical curves. There are two resonant peaks, which are a lot smoother in the measured curves. The frequency of the first resonant peak is same as the SRF of the CM choke, i.e. 1 MHz, whereas the second peak is due to the Y-capacitors' resonance, i.e. about 20 MHz.

The other curves in Fig. 6a) are plots of the theoretically calculated CM IL for $0.1\,\Omega\,/\,100\,\Omega$ and $100\,\Omega\,/\,0.1\,\Omega$ source and load impedances, which correspond to the approximate

worst-case measurements. Unfortunately, such measurements could not be performed due to the lack of equipment with such characteristics.

According Fig. 6a), the CM IL of an EMI filter is lowest when the noise source's impedance is $0.1\,\Omega$ and the filter is terminated with $100\,\Omega$ impedance.

B. DM Insertion Loss

Measuring the DM IL of a power filter requires two transformers as it is shown in Fig. 5b). The attenuation of the transformers without any filter was measured to be only 2-3 dB. Nevertheless, it was subtracted from the DM IL measurements obtained with our filter. The result is plotted in Fig. 6b) as "Measured IL" curve, representing the symmetrical attenuation of the filter under $50\,\Omega\,/\,50\,\Omega$ test conditions.

The theoretically calculated curve for $50\,\Omega\,/\,50\,\Omega$ DM IL is also plotted in Fig. 6b). There are three peaks in the measured and calculated DM IL curves. The first one is at about 2.2 MHz. This was the reason for assuming the unknown SRF of the leakage inductor to be 2.2 MHz. The second peak in the theoretical curve is clearly due to the X-capacitor's SRF at 3.5 MHz. However, in the measured curve, the second peak appears at 16.7 MHz. The third peak in the theoretical curve is due to the Y-capacitor's SRF at about 20 MHz. The unknown and inaccurate model of the leakage inductance, which plays role in the DM attenuation, is probably the main reason for the difference between the theoretical and measured curves.

The other curves in Fig. 6b) are the theoretically calculated DM IL curves corresponding to the approximate worst-case measurements. Up to about 7 MHz these curves overlap each other. Above 18 MHz again the $0.1\,\Omega\,/\,100\,\Omega$ IL is the lowest among all DM IL curves. The peaks encountered in the theoretical curves for the standard DM IL are present in the worst-case curves as well. They appear at the same frequencies, which are the SRFs of the components of the filter.
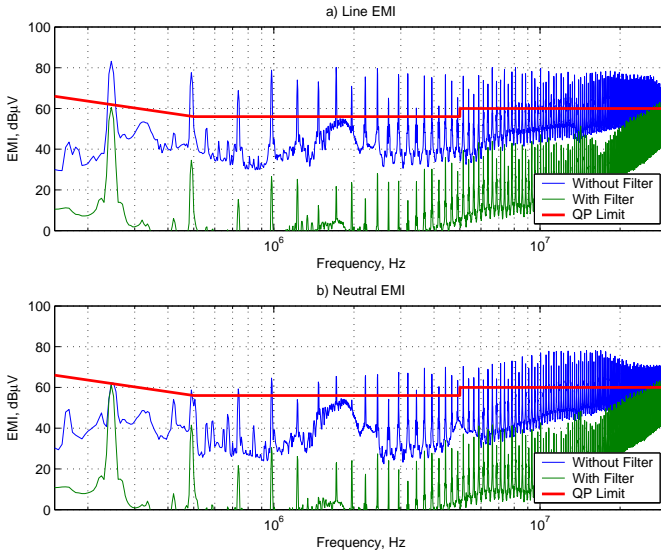
Fig. 7. EMI from a buck converter.

Fig. 9. Measured CM and DM EMI using current probe EZ-17.

V. EMI MEASUREMENTS FROM A BUCK CONVERTER

A. EMI from the Buck Converter without Input Filter

To obtain the actual attenuation, provided by our filter operating with a SMPS, we used a buck converter with switching frequency 250 kHz and output voltage 12 V. The converter was loaded with 1 A load current and supplied with 35 V input voltage. Under these conditions it drew 0.38 A input current from the dc supply.

The measuring principle was shown Fig. 1. Measurements were conducted in accordance with EN 55022 standard [12]. The same EMI test receiver ESCS 30, as in the IL measurements was used. The 50 µH / 50 Ω LISN ESH3-Z5 is also from ROHDE & SCHWARZ.

The EMI from buck's line and neutral wires without input filter was measured using *quasi-peak* (QP) and *average* (AV) detectors. To make the Figures more readable, only the limit
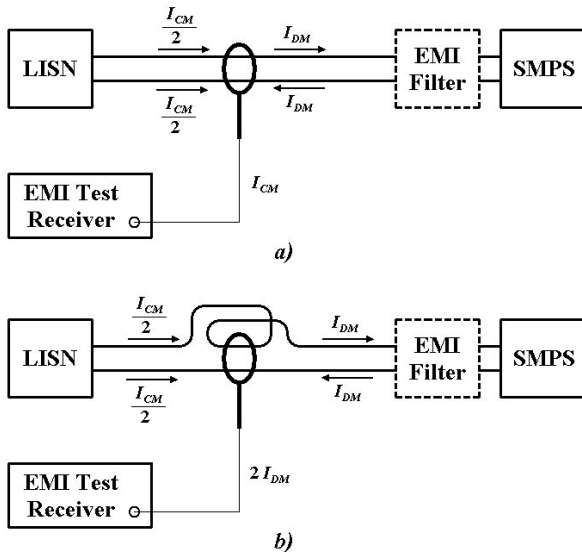

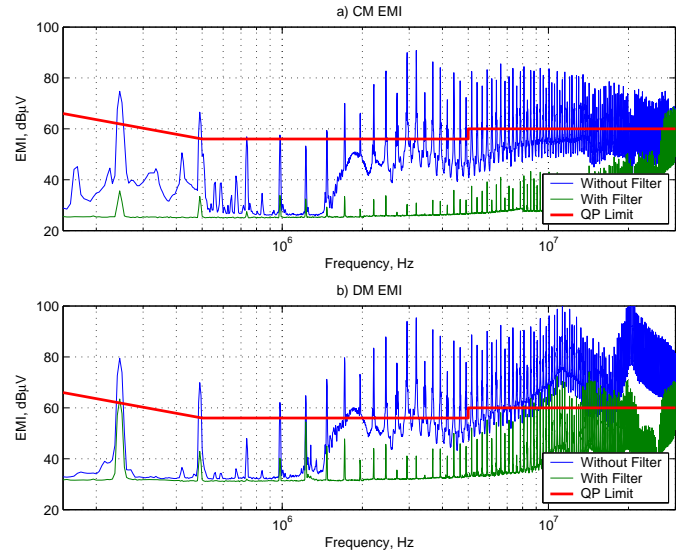Fig. 8. Measuring CM and DM currents with a current probe.

and measurement results for QP detector are plotted. The blue lines in Fig. 7a) and Fig. 7b) show the EMI level from the buck converter, measured from the line and neutral respectively. Clearly the buck converter does not comply with the limit set in the standard.

B. EMI from the Buck Converter with Input Filter

After inserting the input filter between the buck converter and the LISN, the line and neutral EMI were measured again. The results are plotted with green lines in Fig. 7a) and Fig. 7b). Although the EMI is largely attenuated, it still exceeds the limit at some frequencies, i.e. the converter is not EMC compatible. This was not the goal, however. The aim was to find out the actual attenuation of an EMI filter and compare it with the IL data of that filter.

C. Actual Attenuation of the Filter

From the IL measuring principle (Fig. 5) there is a clear distinction between CM and DM IL. To compare them with the actual attenuation, the EMI from the buck converter with and without input filter, need to be divided into its components. The CM noise can be measured by using DM rejection network [13], but the DM noise level would be left unknown. Another alternative would be to use EMI separators [14]-[17], but such devices were not available to us. A third method, presented here, is to measure the CM and DM noise using a current probe.

The measuring principle is shown in Fig. 8. The EMI test receiver measures the CM current, as shown in Fig. 8a), and twice the DM current, as shown in Fig. 8b). The EMI measuring instrument measures the voltage over a 50 Ω resistor and scales it according the equation:

$$EMI = 20 \cdot \lg U \qquad (8)$$

It was shown in Fig. 2c), that because of the LISN, the CM current flows through 25 Ω resistance. Therefore, the CM
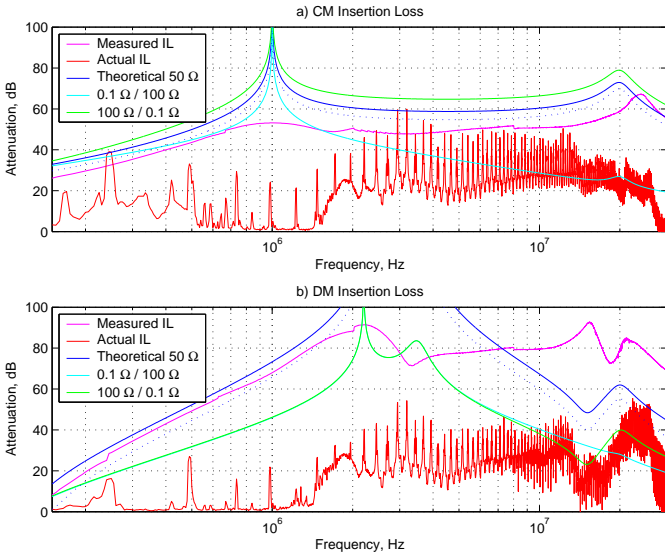
Fig. 10. Actual, standard measured and theoretical insertion loss curves.

EMI is:

$$EMI_{cm} = 20 \cdot \lg(I_{cm} \cdot 25) = 20 \cdot \lg I_{cm} + 20 \cdot \lg 25 \qquad (9)$$

The blue line in Fig. 9a) is a plot of the measured CM current from the buck converter with an added constant according (9), i.e. the CM EMI component. In the same way the CM noise from the buck with input filter is plotted with a green line in Fig. 9a). The difference between these two measurements is the actual CM IL, plotted in Fig. 10a).

$$IL_{cm} = EMI_{cm}^{nf} - EMI_{cm}^{f} = 20 \cdot \lg I_{cm}^{nf} - 20 \cdot \lg I_{cm}^{f} \qquad (10)$$

The minimum current, which can be sensed by the current probe, is the reason for the flat minimum level of the CM EMI in Fig. 9. The constant added to the CM measurement results, according (9), disappears in (10), i.e. for the actual IL what matters is only the difference between the CM currents measured without and with filter inserted.

It was shown in Fig. 8b) that the current probe captures twice the DM noise current. It was also shown earlier that the DM current flows through a 100 Ω resistance. That is why, the DM EMI from the buck converter with and without input filter, plotted in Fig. 9a), can be obtained from:

$$EMI_{dm} = 20 \cdot \lg\left(\frac{2 \cdot I_{dm}}{2} \cdot 100\right)$$
$$EMI_{dm} = 20 \cdot \lg(2 \cdot I_{dm}) + 20 \cdot \lg 50 \qquad (11)$$

The actual DM attenuation is again the difference between the measurements of the DM currents without and with input filter:

$$IL_{dm} = EMI_{dm}^{nf} - EMI_{dm}^{f} = 20 \cdot \lg I_{dm}^{nf} - 20 \cdot \lg I_{dm}^{f} \qquad (12)$$

The actual DM attenuation, obtained according (12), is plotted in Fig. 10b).

The actual CM IL overlaps the theoretical CM IL curve for 0.1 Ω / 100 Ω source and load impedance, except for the frequencies above 500 kHz up to 2 MHz. The actual DM IL is close to the theoretical DM IL curve for 100 Ω / 0.1 Ω, except from 500 kHz up to 7 MHz.

The differences between the theoretical and actual IL can be due to measurement errors, e.g. sensitivity limit of the current probe. Another reason is that the filter cannot attenuate more EMI than there is available. For example, if there is a filter with 80 dB attenuation, but the noise is only 40 dB, the actual attenuation cannot exceed 40 dB.

VI. CONCLUSIONS

Based on the results and calculations, it can be concluded that the "approximate worst case" IL data are the right source of information for the designer selecting power line filters for SMPS.

The CM attenuation of a passive EMI filter, operating with a SMPS is most likely to be about the magnitude of the IL data of that filter for 0.1 Ω / 100 Ω conditions.

The DM attenuation of a passive EMI filter, operating with a SMPS can be expected to be about the level of the filter's IL data for 100 Ω / 0.1 Ω source and load impedance conditions.

If the approximate worst-case IL measurements data are not available, the designer has no other choice, but to use the usual 50 Ω / 50 Ω IL data. However, the actual IL can be a lot lower than those data.

During the selection process the designer should not forget the interactions between the EMI filter and the SMPS. To avoid them, the power filter's output impedance must be a lot smaller than the SMPS's input impedance, and the resonant frequencies of the input filter and output filter of the SMPS should be as far apart as possible.

REFERENCES

[1] L. Tihanyi, *Electromagnetic Compatibility in Power Electronics*, IEEE Press, Inc., 1995, pp. 403.
[2] R. L. Ozenbaugh, *EMI Filter Design,* Marcel Dekker, Inc., 1996, pp. 252.
[3] CISPR 17 Measurements, Application Note 690-264A, Schaffner, 1996.
[4] W.-K. Chen, *et al.*, *The Circuits and Filters Handbook*, IEEE Press, Inc., 1995, pp. 2861.
[5] K. S. Kostov, J. Kyyrä, and T. Suntio, "Analysis and Design of EMI Filters for DC-DC Converters Using Chain Parameters", *European Power Electronics Conference*, Toulouse, September, 2003.
[6] *MKP 336 2 X2, Interference Suppression Film Capacitors*, Vishay BCcomponents, April, 2004.
[7] *MKP 336 6 Y2, Interference Suppression Film Capacitors*, Vishay Bccomponents, August, 2003.
[8] *136 RVI, Aluminum Electrolytic Capacitors, Radial, Very Low Impedance*, Bccomponents, January, 2000.
[9] *EMC Components*, Publication 690-626B, Schaffner, 2001.
[10] *RFI / EMI Filters*, Publication 690-057A, Schaffner, 1994.
[11] *EMI Test Receiver ESCS 30*, Operating Manual 1102.4568.12-01.

[12] *Information Technology Equipment – Radio Disturbance Characteristics – Limits and Methods of Measurement*, EN 55022 Standard, 2003.

[13] M. L. Nave, *Power Line Filter Design for Switch-Mode Power Supplies*, Van Nostrand Reinold, 1991, pp. 210.

[14] T. V. Rauner, "A Measurement System for Evaluation of the Coupling Modes and Mechanisms of Conductive Noise", Master's Thesis, Helsinki University of Technology, 1997, pp. 64.

[15] C. R. Paul and K. B. Hardin, "Diagnosis and Reduction of Conducted Noise Emissions", IEEE Transactions on Electromagnetic Compatibility, vol. 30, pp. 553-560, November 1988.

[16] T. Guo, D. Y. Chen, and F. C. Lee, "Separation of the Common-Mode and Differential Mode Conducted EMI Noise", *IEEE Transactions on Power Electronics*, vol. 11 , pp. 480-488, May 1996.

[17] M. C. Caponet, F. Profumo, L. Ferraris, A. Bertoz, and D. Marzella, "Common and Differential Mode Noise Separation: Comparison of two Different Approaches", *IEEE 32nd Annual Power Electronics Specialists Conference*, vol. 3, pp. 1383–1388, June 2001.